

Molecular details of various biochemical and biological processes can be investigated and monitored *in vitro* and *in vivo* by various fluorescent methods because of the inherent sensitivity, specificity, and temporal resolution of fluorescence spectroscopy. The combination of fluorescence spectroscopy with flow and image cytometry has provided a solid basis for rapid and continuous development in these technologies. In order to utilize these techniques properly, cytometrists must be familiar with the working principles of the instruments and also with the basic concepts of fluorescence spectroscopy. This unit focuses on a special phenomenon of fluorescence spectroscopy, namely fluorescence resonance energy transfer (FRET). FRET is a radiationless process in which energy is transferred from an excited donor to an acceptor molecule under favorable spectral and orientational conditions. These conditions will be discussed in detail below. FRET processes during fluorescence measurements in flow and image cytometry can either compromise results or open new applications for these techniques. In order to distinguish between the adverse and beneficial effects of FRET, one must understand the theoretical background of the phenomenon. When multiple fluorescent probes are simultaneously applied, the possible cross-talk between fluorescent dyes (e.g., FRET processes) should be ruled out, or controlled if one wants to quantitate the cell-surface expression of various antigens at the same time. In contrast to this adverse effect, FRET can also be used to improve the spectral characteristics of fluorescent dyes and dye combinations, such as the tandem dyes in flow and image cytometry and FRET primers in DNA sequencing and the polymerase chain reaction. The driving force in these applications is the use of single-wavelength excitation while providing various dye combinations with a wide range of Stokes shifts to make possible the simultaneous detection of three or four fluorescent dyes. Combination of FRET with monoclonal antibodies has led to a boom in structural analysis of proteins in solution and also in biological membranes. Analysis based on functional heterogeneity of leukocytes is accompanied by analysis based on specific expression of various cell-surface antigens. International work-

shops assign a “cluster of differentiation” (CD) nomenclature to these antigens, based on reactivity with groups of monoclonal antibodies. Cell-surface mapping of CD molecules on immunocompetent cells has attracted more and more interest in the last three decades. Experiments revealing the structure of these antigens have led to the discovery, among others, of the immune synapse (Bhatia et al., 2005; Cemerski and Shaw, 2006). With the help of FRET, molecular dimensions can be measured and determined in functioning, living cells, providing information that would be impossible to obtain with other classical approaches—e.g., with X-ray crystallography.

This unit describes the theory behind FRET, characterizes available parameters and instruments, discusses limitations, and provides a few examples of the application of FRET.

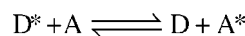
## THEORY OF FRET

FRET was first observed by Perrin at the beginning of the 20th century, but it was Theodor Förster who proposed a correct theory describing long-range dipole-dipole interactions between fluorescent molecules, more than 50 years ago (Förster, 1946, 1948). He derived an equation that relates FRET efficiency to the spectroscopic parameters of fluorescent dyes. His ingenious discovery that fluorescence dipole-dipole interaction depends, in addition to orientation and other spectroscopic parameters, on the negative sixth power of the distance between the dipoles furnished one of the most sensitive methods for measuring atomic and molecular distances at the nanometer level. After the theoretical background of the FRET process was illuminated, it took decades before FRET technology gained wide application in chemistry, biochemistry, and cell biology.

FRET is a physical process in which energy is transferred from an excited donor molecule to an acceptor molecule by means of intermolecular long-range dipole-dipole coupling. One of the most important factors influencing the strength of coupling is the distance between the donor and acceptor molecules. Energy transfer occurs in the 1- to 10-nm distance range with measurable efficiency, and these distances correlate well with macromolecular dimensions (Stryer, 1978). Energy transfer is

nonradiative—i.e., the donor does not actually emit a photon and the acceptor does not absorb a photon. The so-called “trivial” radiative energy transfer has very low probability at low concentrations ( $<10^{-6}$  M) of the fluorescent probes.

In order to explain the mechanism of fluorescence resonance energy transfer, let us consider a system with two different fluorophores where the molecule with higher energy absorption is defined as the donor (D) and the one with lower energy absorption as the acceptor (A). If the donor is in an excited state, it will lose energy by internal conversion without emission, until it reaches the ground vibrational level of the first excited state (Kasha’s rule; see Fig. 1.12.1). If the donor emission energies overlap with the acceptor absorption energies, the following resonance can occur through weak coupling:



**Equation 1.12.1**

where D and A denote the donor and the acceptor molecules in the ground state, while  $D^*$  and  $A^*$  denote the excited states of the fluorophores. The rate of the forward process is  $k_T$ , while the rate of the inverse process is  $k_{-T}$ . Since vibrational relaxation converts the excited acceptor to the ground vibrational level, the inverse process is highly unlikely to occur (Fig. 1.12.1). As a result, the donor

molecules become quenched, while the acceptor molecules become excited and, under favorable conditions, can emit fluorescent light with their own quantum yield. This latter process is called sensitized emission (Fig. 1.12.2).

The efficiency ( $E$ ) of FRET is a quantitative measure of the number of quanta that are transferred from the donor to the acceptor and can be expressed as

$$E = \frac{\text{no. quanta transf. from donor to acceptor}}{\text{no. quanta abs. by donor}}$$

**Equation 1.12.2**

According to the theory of Förster, the rate ( $k_T$ ) and efficiency ( $E$ ) of energy transfer can also be written as

$$k_T = \text{const } k_F J n^{-4} R^{-6} \kappa^2$$

**Equation 1.12.3**

$$E = \frac{k_T}{k_T + k_F + k_D}$$

**Equation 1.12.4**

where  $k_F$  is the rate constant of fluorescence emission of the donor and  $k_D$  is the sum of the rate constants of all other deexcitation processes of the donor.  $R$  is the separation distance between the donor and acceptor molecules, and  $\kappa^2$  is an orientation factor which is a function of the relative orientation

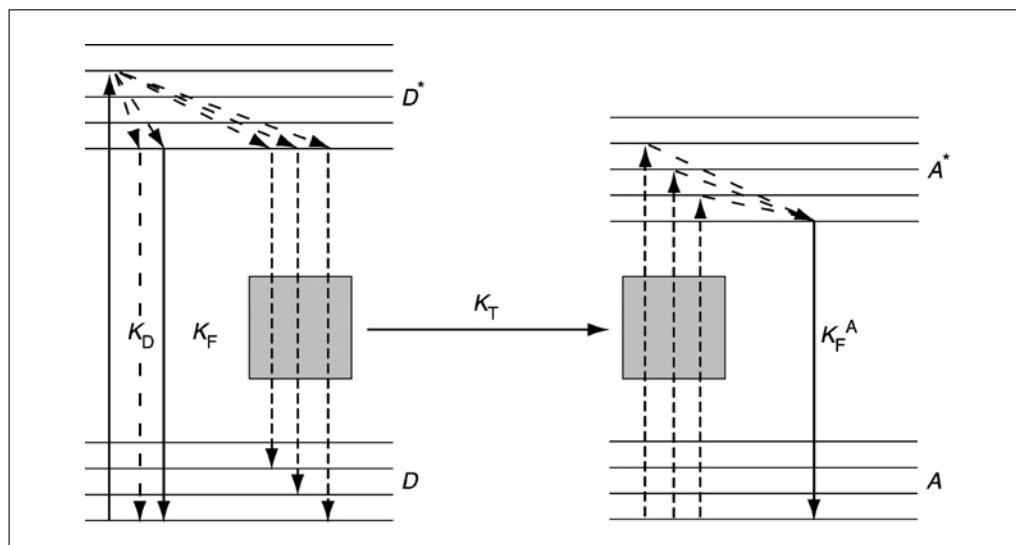


**Figure 1.12.1** The energy balance of the FRET phenomenon. The donor molecule is excited to a higher vibrational level of the first excited state, from which it decays to the lowest vibrational level according to Kasha’s rule. From this state it can relax to ground state through fluorescence or internal conversion, or via energy transfer ( $k_T$  arrow). Only those transitions that have the matching pair in the energy diagram of the acceptor take part in this process. The acceptor decays to the ground state through similar mechanisms.

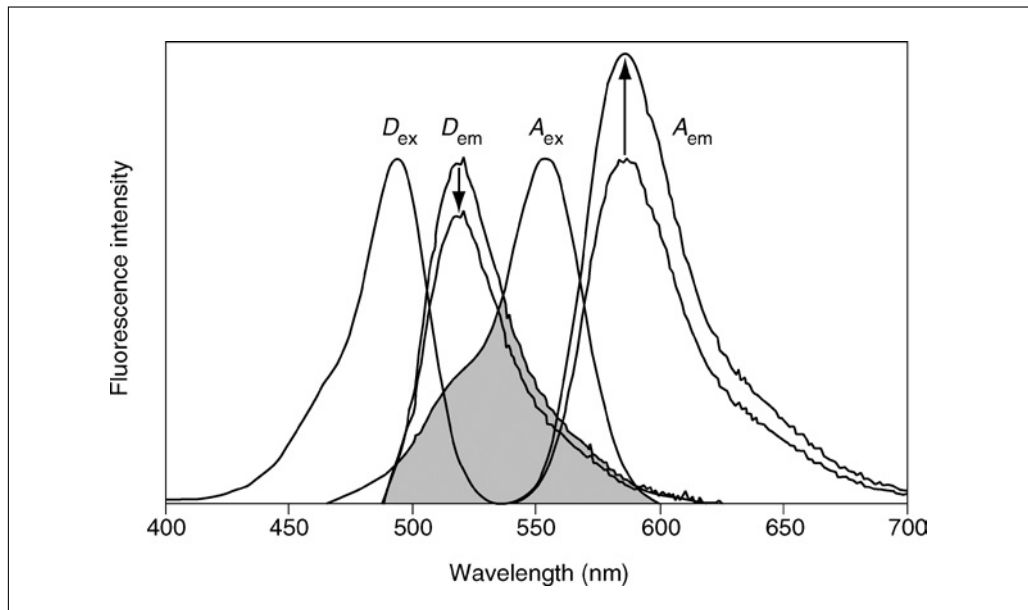


**Figure 1.12.2** Fluorescence excitation and emission spectra of a suitable FRET pair: fluorescein (donor) and tetramethylrhodamine (acceptor). The shaded area represents the overlap integral ( $J$ ). The spectra are normalized for display purposes. The downward-pointing arrow indicates the quenching of the donor, whereas the upward-pointing arrow shows the sensitized emission of the acceptor. The amount of quenching and sensitized emission is distorted for demonstrational purposes.

of the donor's emission dipole and the acceptor's absorption dipole in space. Other parameters are  $n$ , the refractive index of the medium, and  $J$ , the spectral overlap integral, which is proportional to the overlap in the emission spectrum of the donor and the absorption spectrum of the acceptor

$$J = \frac{\int F_D(\lambda) \epsilon_A(\lambda) \lambda^4 d\lambda}{\int F_D(\lambda) d\lambda}$$

**Equation 1.12.5**

where  $F_D(\lambda)$  is the fluorescence intensity of the donor at wavelength  $\lambda$  and  $\epsilon_A(\lambda)$  is the molar extinction coefficient of the acceptor.

For dipole-dipole vectorial interaction, the transition dipoles of the donor and the acceptor in space must be oriented favorably relative to each other as given by the following equation

$$\kappa = (\cos\alpha - 3\cos\beta\cos\gamma)^2$$

**Equation 1.12.6**

where  $\alpha$  is the angle between the transition moments of the donor and the acceptor, and  $\beta$  and  $\gamma$  are the angles between the line joining the centers of the fluorophores and the transition moments of the donor and acceptor, respectively (Fig. 1.12.3). From theoretical con-

siderations,  $\kappa^2$  is in the range between 0 and 4. Uncertainties in the value of  $\kappa^2$  cause the greatest error in distance determination by energy transfer. Fortunately,  $R$  depends on  $(\kappa^2)^{1/6}$ , so that it changes only slightly over a wide range (e.g., 0.3 to 3) of  $\kappa^2$ . Direct measurement of the value of  $\kappa$  is impossible; however, fluorescence anisotropy measurements on donor and acceptor molecules can be performed to limit possible values of the factor, but rarely do they eliminate all of the uncertainty (Dale, 1979). In addition, if the donor or the acceptor or both have a certain degree of rapid rotational freedom,  $\kappa^2$  becomes 2/3, owing to the random movement and orientation of the donor and the acceptor. This condition is usually satisfied for fluorophores attached to biomolecules at the cell surface (Dale, 1979).

It can be shown that

$$E = \frac{R_0^6}{R^6 + R_0^6}$$

**Equation 1.12.7**

From Equations 1.12.3, 1.12.4, and 1.12.7 it follows that

$$k_T = \frac{1}{\tau} \left( \frac{R_0}{R} \right)^6$$

**Equation 1.12.8**

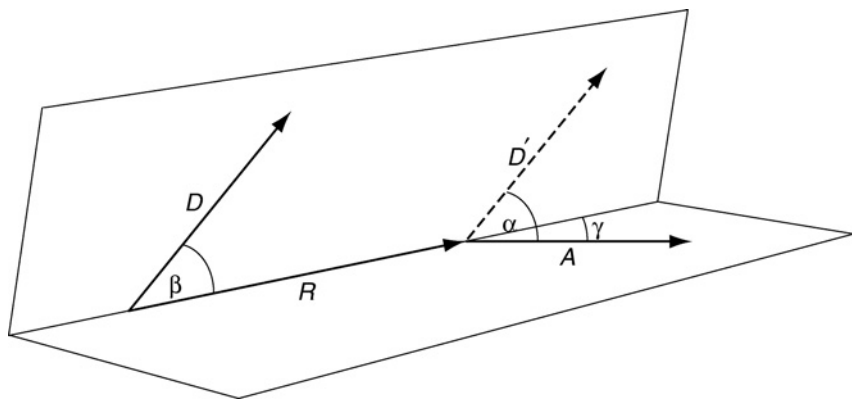


**Figure 1.12.3** The orientation of the emission dipole of the donor (D) and the absorption dipole of the acceptor (A).  $R$  is the distance between the two dye molecules.  $\alpha$  is the angle of the two dipoles,  $\beta$  is the angle between the transition moment of the donor and the line joining the two dyes, while  $\gamma$  is the angle between the transition moment of the acceptor and the line joining the two dyes.

where  $\tau$  is the donor's lifetime in the absence of the acceptor, and  $R_0$  is the characteristic distance between the donor and the acceptor when the transfer efficiency is 50%. Also consider the equation

$$R_0 = \text{const} (J \kappa^2 Q_D n^{-4})^{1/6}$$

**Equation 1.12.9**

In this equation  $Q_D$  is the quantum efficiency of the donor in the absence of the acceptor. To observe effective transfer in the 1- to 10-nm range, the fluorescence emission spectrum of the donor and the absorption spectrum of the acceptor should overlap adequately, and both the quantum yield of the donor ( $Q_D$ ) and absorption coefficient of the acceptor ( $\epsilon_A$ ) should be sufficiently high ( $Q_D \geq 0.1$  and  $\epsilon_A \geq 1000 \text{ M}^{-1}\text{cm}^{-1}$ ).

### DETERMINATION OF FÖRSTER DISTANCE ( $R_0$ )

FRET efficiency measurements are most sensitive to distance variation when the separation of the donor and acceptor is close to the  $R_0$  (Förster) distance. Thus, when choosing a donor-acceptor pair, the molecular dimensions of the system to be studied should be considered. Since there is no internal distance reference in fluorescence resonance energy transfer, all distances calculated from transfer efficiencies are relative to an  $R_0$  distance evaluated from spectroscopic properties of the donor and acceptor.  $R_0$  thus provides a reference ruler in distance measurements. Even to

estimate the adverse effect of FRET, the  $R_0$  value of the donor-acceptor pair in question must still be determined in order to determine the effective range of the FRET process. Owing to error propagation, it is almost impossible to measure FRET efficiencies of <5% accurately; therefore, the maximal distance at which FRET can be measured is  $1.63 \times R_0$ . This relatively short distance range is due to the fact that the rate of FRET depends upon the inverse sixth power of the distance between the donor and acceptor (Fig. 1.12.4).

Calculation of  $R_0$  for a donor-acceptor pair requires knowledge of (1) the molar absorption coefficient and the absorption spectrum of the acceptor, (2) the fluorescence emission spectrum of the donor, and (3) the quantum yield ( $Q_D$ ) of the donor. The absorption coefficient of the acceptor is usually given at least for one wavelength, and the absorption spectrum can easily be obtained using any commercially available spectrophotometer. The fluorescence emission spectrum of the donor can be determined with a spectrofluorimeter; however, the spectrum usually contains a wavelength-dependent instrument response. The true emission spectrum can be determined with instruments in which manufacturers provide instrument-response correction. Alternatively, reference compounds with known emission spectra can be used for calibrating the instrument. Similarly,  $Q_D$  can be determined using reference compounds with known quantum yields, such as quinine in 0.1 N  $\text{H}_2\text{SO}_4$ , with  $Q = 0.55$ , or fluorescein in 0.1 N  $\text{NaOH}$ , with  $Q = 0.92$ . Knowing of the

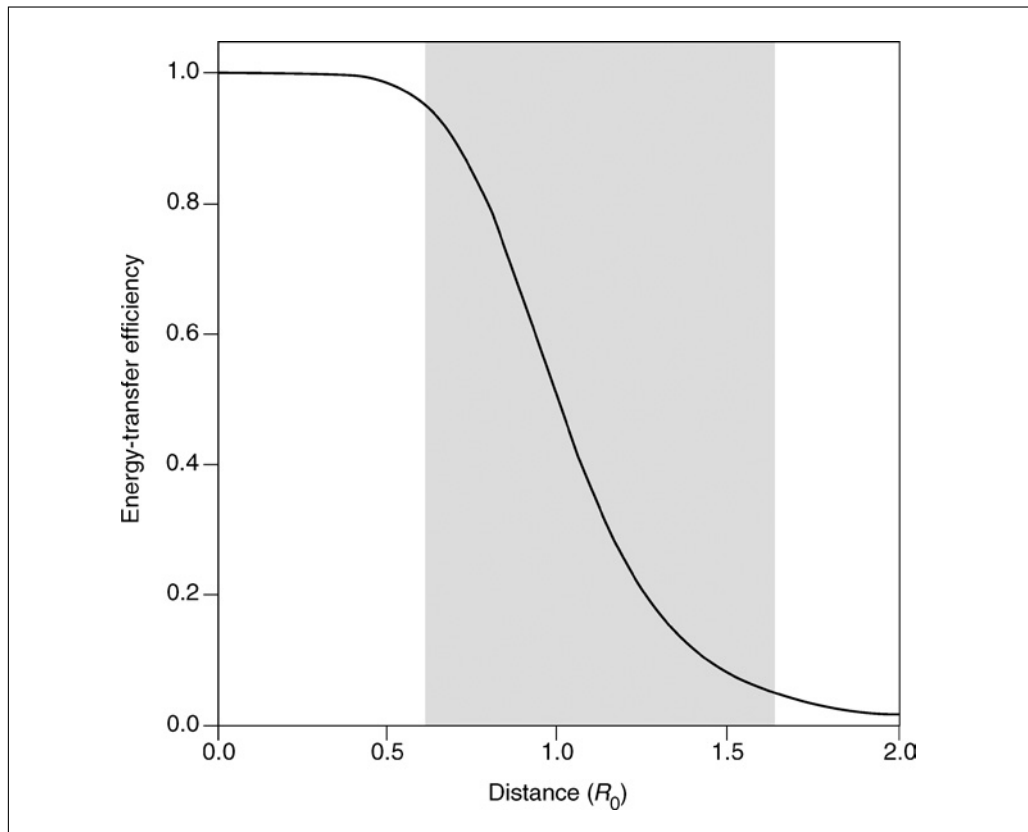


**Figure 1.12.4** Distance dependence of the energy transfer efficiency. Distances are expressed in  $R_0$  units. The shaded area shows the useful distance range, where the energy transfer efficiency is between 0.95 and 0.05, meaning  $(0.61 \times R_0)$  to  $(1.63 \times R_0)$ . Note that the curve is asymmetrical.

absorption spectrum of the acceptor and the true emission spectrum of the donor, the overlap integral ( $J$ ) can be calculated according to Equation 1.12.5. After  $J$  and  $Q_D$  have been determined,  $R_0$  can be calculated, assuming  $n = 1.33$  for aqueous solution and  $\kappa^2 = 2/3$  for random dipole orientation, according to Equation 1.12.9. Since quantum yield and spectral shape may be environment sensitive,  $R_0$  distances may vary as solution conditions change. A selected list of  $R_0$  distances for donor-acceptor pairs applied in flow and image cytometric measurements is shown in Table 1.12.1. A comprehensive and useful list of  $R_0$  values for over 70 donor-acceptor pairs is provided by Wu and Brand (1994). The largest  $R_0$  value reported for a single donor-acceptor pair is 8.0 nm for the rhodamine B-malachite green dye pair (Yamazaki et al., 1990). The use of molecules that have clusters of acceptors with high molar absorption coefficient for each acceptor can extend the  $R_0$  value. Along this line, Mathis reported an exceptionally large  $R_0$  of 9.0 nm using europium cryptate as donor and allophycocyanin as acceptor (Mathis, 1993). When applying phycobilin proteins, it should be kept in mind that these molecules have

bulky dimensions, which can interfere with the original goal, i.e., with accurate distance measurements. For those taking interest in  $R_0$  values for various green fluorescent protein (GFP) analogs, an accurate and comprehensive analysis of green fluorescent protein pairs is given in Patterson et al. (2000). This paper also provides  $R_0$  values for possible homo-transfers (i.e., FRET between spectroscopically identical molecules).

## HOW TO MEASURE FRET EFFICIENCY

The energy transfer efficiency, as follows from the above formulas, can be determined in a number of different ways. Since energy is transferred from the excited donor to the acceptor, the lifetime ( $\tau$ ), quantum efficiency ( $Q$ ), and fluorescence intensity ( $F$ ) of the donor decrease, if the acceptor is present (Equation 1.12.10). As a consequence, the fluorescence intensity of the acceptor increases (sensitization) if the donor is present (Equation 1.12.11).

$$1 - E = \frac{\tau_D^A}{\tau_D} = \frac{F_D^A}{F_D} = \frac{Q_D^A}{Q_D}$$

**Equation 1.12.10**

**Table 1.12.1** Characteristic  $R_0$  Values for Selected Donor-Acceptor Pairs<sup>a,b</sup>

Donor ( $\lambda_{\text{ex}}/\lambda_{\text{em}}$ )	Acceptor ( $\lambda_{\text{ex}}/\lambda_{\text{em}}$ )	$R_0$ (nm)	References
FCA (400/470)	PI in DNA (540/620)	3.0	Szöllősi et al., 1978
IAF (490/515)	DiI-C <sub>18</sub> (546/565)	3.5	Shahrokh et al., 1991
DAPI (350/470)	EB (510/595)	3.7	Maliwal et al., 1995
IAF (490/515)	TMR (557/576)	3.7	Taylor et al., 1981
BFP (389/440)	GFP (488/511)	4.0	Mahajan et al., 1998
IAEDANS (336/490)	IAF (490/515)	4.4	Gettins et al., 1990
RLUC (-/475)	EYFP (480/530)	5.0	Xu et al., 1999
Cy3 (554/568)	Cy5 (649/666)	5.0	Bastiaens and Jovin, 1996
CF (490/525)	Texas red (596/620)	5.1	Johnson et al., 1993
5(6)-CF (490/517)	5(6)-CF (490/517)	5.1-5.7	Chen and Knutson, 1988
TMR (557/576)	Texas red (596/620)	5.2	Ha et al., 1996
Fluorescein (490/525)	EITC (525/545)	5.4	Carraway et al., 1989
C <sub>18</sub> -Rh (560/590)	C <sub>18</sub> -Rh (560/590)	5.5-5.8	MacDonald, 1990
Fluorescein (490/525)	TMR (557/576)	5.6	Kosk-Kosicka et al., 1989
NBD (450/530)	LRH (575/595)	5.6	Wolf et al., 1992
AO in DNA (502/526)	Crystal violet (596/-)	7.0	Maliwal et al., 1995
BPE (480-565/578)	CY5 (649/666)	7.2	Ozinskas et al., 1993
Rhodamine B (540/625)	MG (630/-)	8.0	Yamazaki et al., 1990
TBP(Eu <sup>3+</sup> ) (307/620)	APC (650/661)	9.0	Mathis, 1993

<sup>a</sup> $\lambda_{\text{ex}}/\lambda_{\text{em}}$ , wavelengths of excitation/emission in nm.

<sup>b</sup>Abbreviations: AO, acridine orange; APC, allophycocyanin; BFP, blue fluorescent protein; BPE, B-phycoerythrin; CFSE, carboxyfluorescein succinimidyl ester; 5(6)-CF, 5(6)-carboxyfluorescein; C<sub>18</sub>-Rh, octadecylrhodamine B; Cy3, sulfoindocyanine dye Cy3.29-OSu; Cy5, sulfoindocyanine dye Cy5.29-OSu; DAPI, 4',6-diamidino-2-phenyl indole; DiI-C<sub>18</sub>, 1,1'-dioctadecyl-3,3',3'-tetramethyl-indocarbocyanine; EB, ethidium bromide; EITC, eosin-5'-isothiocyanate; EYFP, enhanced yellow fluorescent protein; FCA, fluorescamine; GFP, green fluorescent protein; IAEDANS, 5-(((2-iodoacetyl)amino)ethyl)amino)naphthalene-1-sulfonic acid; IAF, 5-iodoacetamido fluorescein; LRH, lissamine rhodamine; MG, malachite green; NBD, 7-nitro-2,1,3-benzoiazol-4-yl (also known as 7-nitrobenz-2-oxa-1,3-diazole); PI, propidium iodide; RLU, *Renilla* luciferase; TBP(Eu<sup>3+</sup>), Eu<sup>3+</sup> trisbipyridine diamine; TMR, tetramethyl rhodamine.

$$\frac{F_A^D}{F_A} = 1 + \left( \frac{\epsilon_D C_D}{\epsilon_A C_A} \right) E$$

**Equation 1.12.11**

In the above equations, the lower indices refer to the donor (D) or acceptor (A), while the upper indices indicate the presence of the donor (D) or the acceptor (A) in the system.  $C_D$  and  $C_A$  are the molar concentrations, while  $\epsilon_D$  and  $\epsilon_A$  are the molar absorption coefficients of the donor and the acceptor, respectively.  $E$  is the efficiency of the energy transfer.

FRET can be determined by measuring the fluorescence characteristics of the donor or the acceptor. Fluorescence intensity, quantum yield, or fluorescence lifetime of the donor changes upon FRET. The simplest way to measure energy transfer is to determine the

decrease in the fluorescence of the donor in the presence of the acceptor. The fractional decrease in the donor fluorescence with the acceptor present is equal to the efficiency of FRET. Fluorescence lifetime measurements are not widely applied for monitoring FRET efficiency because time-resolved fluorescence measurements require sophisticated and expensive instruments. Interestingly, no FRET data between membrane proteins determined by flow cytometric lifetime measurements have been published to date, although flow cytometers capable of fluorescence lifetime measurements have been constructed and characterized (Crissman and Steinkamp, 2001). As greater progress is made in image cytometry, more and more papers are being published in which FRET efficiency values are determined by applying fluorescence lifetime imaging

(FLIM) microscopy (Wallrabe and Periasamy, 2005; Waharte et al., 2006).

Although it is not necessary to have a fluorescent acceptor, the observation of the increased emission of the acceptor is an important confirmation of energy transfer, because it arises only from FRET, whereas donor quenching can arise from several trivial sources. In an ideal case, where a system is excited at the excitation maximum of the donor and the fluorescence detected at the emission maximum of the acceptor, we can detect fluorescence only if both donor and acceptor molecules are present and there is FRET between them. (Donor-only and acceptor-only samples will not produce measurable fluorescence intensities under these ideal conditions.) Generally, the donor has a tail in the emission spectrum contributing to the fluorescence intensities at the emission maximum of the acceptor. In addition, most acceptors have some absorption at the excitation wavelength of the donor. Hence, the calculation of energy transfer efficiency is more complicated owing to these correction factors. The spectral overlap between the donor's fluorescence and the acceptor's own fluorescence should be taken into account when calculating the FRET efficiency.

In addition to methods involving the quenching of the donor and the sensitization of the acceptor, FRET efficiency can be determined using time-resolved or steady-state anisotropy measurements. These measurements entail quantitation of the anisotropy increase of the donor in the presence of an acceptor dye due to the decreased fluorescence lifetime of the donor (Matkó et al., 1993; Damjanovich et al., 1997). On the other hand, anisotropy may decrease when FRET occurs between the same molecules in identical environments (homo-transfer), possibly due to a change in fluorophore orientation, whereas there is no change in the fluorescence intensity or the lifetime of the dyes. The efficiency of homo-transfer can be determined only with fluorescence anisotropy measurements. Utilizing the so-called energy-migration FRET, the degree of homo-association of visible fluorescent proteins was determined without the necessity of two independent transfections in the same cell (Lidke et al., 2003). With the help of a more elaborate version of flow cytometric fluorescence homo-transfer measurements, the existence of receptor trimers on the cell surface of immunocompetent cells was detected (Bene et al., 2005).

Another possibility for determining the energy transfer efficiency is based on the altered photobleaching rate of the donor in the presence of acceptor. Although photobleaching should usually be minimized, it can in some cases actually be exploited to measure FRET efficiency. Photobleaching of the donor occurs only when it is in the excited state; before de-excitation occurs, there is some probability that photobleaching will remove that fluorophore from the excited state by destroying its molecular structure. The excited-state reactions are instrumental in photobleaching processes. The donor photobleaches more slowly if energy transfer to an acceptor occurs, since energy transfer is an alternative pathway for the excited-state relaxation. It can be shown that the fractional increase in the photobleaching time constant is the same as the fractional decrease in the fluorescence lifetime of the donor (Jovin and Arndt-Jovin, 1989a, b). The efficiency of FRET can be determined by comparing the bleaching rate of the donor in the presence and absence of acceptor (Jovin and Arndt-Jovin, 1989a,b; Nagy et al., 1998a,b). A computer program for analyzing photobleaching FRET image series has been published recently (Szentesi et al., 2005). A new variant of donor-photobleaching FRET has been introduced where the efficiency of FRET is determined from the kinetics of the photobleaching of the acceptor, which has been sensitized by a donor. This technique utilizes dye combinations in which the acceptor bleaches much faster than the donor, even when only the donor is excited. This donor-mediated acceptor-photobleaching FRET allows the measurement of FRET efficiencies with exceptional accuracy (Mekler, 1997).

In another approach, the acceptor is directly excited and bleached at its absorption maximum, and the intensity of the donor is compared before and after the photodestruction of the acceptor (Bastiaens et al., 1996; Vereb et al., 1997). A detailed description of the acceptor photobleaching method has been given elsewhere (Vereb et al., 2004), and a protocol for FRET measurements utilizing acceptor photobleaching is described in *UNIT 12.7*. The list of methods for FRET measurement discussed above is far from complete. For imaging FRET, 22 different methods have been described recently. Jares-Erijman and Jovin (2003) have created an impressive catalog of FRET microscopy methods in their review, providing a systematic classification and characterization of 22 possible approaches. In

## Flow Cytometry Instrumentation

### 1.12.7

addition to the FRET methods used already, several new and exotic strategies have been suggested with potential for implementation in fluorescence microscopy (Jares-Erijman and Jovin, 2003).

While there are currently 22 different ways of assessing FRET, the literature includes many papers applying a 23rd method, which is a simple but highly incorrect and unreliable approach based on exciting the donor and detecting acceptor emission. So-called FRET images are taken using filter sets specifically sold for this purpose. The assumption made is that the stronger the signal, the more efficient FRET is at a given pixel. However, the signal obtained in the acceptor channel upon excitation at the donor absorption maximum will actually consist of four components, varying individually from pixel to pixel: the quantity of the donor fluorophore and its emission leaking into the acceptor channel; the quantity of the acceptor fluorophore and its emission upon excitation in the donor absorption regime; the efficiency of FRET convolved with the quantity of both the donor and acceptor fluorophores; and, finally, the autofluorescence. It follows that labeling conditions, expression of protein targets for donor and acceptor labeling (or donor and acceptor fluorescent proteins), and fluorescent metabolites produced by the cell will greatly influence the signal registered from each cell and even from each pixel, making the FRET signal only a component of what is detected, and with a contribution weight that is difficult to determine. It is thus not sufficient to take such FRET images, but donor and acceptor signals that would be present in the absence of FRET must also be estimated by acquiring images with donor- and acceptor-specific fluorescence filter sets, and determining the spectral spillage factors (and possibly also the autofluorescence contribution) from single-labeled samples (see protocols described in *UNIT 12.8*).

### CHOICE OF INSTRUMENT FOR FRET MEASUREMENT

When designing a FRET study, the first question to consider is whether the biological problems are best addressed by spectrofluorimetry, flow cytometry, or imaging microscopy. Spectrofluorimetry is often much easier to implement than quantitative flow cytometry or imaging-microscopy studies, despite the advances in instrumentation and software. Usually, donor quenching or acceptor sensitization is measured in this approach. In spectrofluorimetry, the cells can be either in

suspension or attached to a coverslip held at an angle to the incident beam. Average fluorescence intensity for thousands of cells can be rapidly measured by these methods. A complete set of samples for FRET efficiency determination should contain at least one unlabeled, two single-labeled (one labeled with donor only, and one labeled with acceptor only), and one double-labeled sample (labeled with donor and acceptor simultaneously). The measured fluorescence intensities must be corrected for light scattering and autofluorescence using the unlabeled sample. At the same time, the fluorescence intensities should be normalized to the same donor and acceptor concentration. For both corrections, very accurate sample preparation is required; cell concentration should be carefully controlled. Another possible source of error is the contribution to the specific fluorescence signal from unbound fluorophores and cell debris. This is very difficult, if not impossible, to control, especially if the fluorescent label has a low binding constant. Multiple washings decrease the contribution of free fluorophores to the fluorescence intensity, but unavoidably increase the amount of cell debris. Another problem is that some cells may become extremely bright during fluorescent labeling (e.g., dead cells in some immunofluorescence experiments). Some potential problems occurring in spectrofluorimetry could be less serious in flow cytometry or microscopy. Distortion caused by dead cells, free dye, or debris can be avoided, and uncertainties in cell concentration do not cause a problem owing to the cell-by-cell type measurement. These are easily excluded in analyses of flow cytometry data or in selecting fields for analysis by microscopy. A detailed comparison of energy transfer measurements in spectrofluorimetry and flow cytometry is described in several references (Mátyus, 1992; Szöllősi et al., 1994; Trón, 1994).

Flow cytometry can provide quantitative measurements on thousands of individual cells, allowing convenient determination of the distribution of fluorescence intensities and energy transfer values in a population. To achieve a high rate of analysis, cells should be in suspension, meaning that cells growing attached to a substrate should be detached mechanically or enzymatically for flow cytometric measurements. These treatments can interfere with the cellular parameters to be investigated. In flow cytometry, donor quenching cannot be used to determine transfer efficiency on a cell-by-cell basis; because the expression levels of various proteins have broad distributions, the

donor intensity cannot be measured in the absence and presence of acceptor on the same cell. (For mean values, donor quenching can also be used as in spectrofluorimetric measurements to provide a single mean FRET efficiency value for the whole cell population.) Sensitized emission of the acceptor, however, can be applied to calculate the transfer efficiency on a cell-by-cell basis, since with multiple excitations the direct and sensitized emissions of the acceptor can be determined on the same cell. As with spectrofluorimetry, four samples are needed for FRET measurements. Unlabeled cells are used for autofluorescence correction, cells labeled with donor only for determining spectral overlap correction factor, and cells labeled with acceptor only for determining the correction factor for direct excitation of the acceptor; cells labeled with both donor and acceptor are used for calculation of the FRET efficiency on a cell-by-cell basis. In flow cytometric measurements, there are three unknown fluorescence parameters: the unquenched donor intensity, the nonenhanced acceptor intensity, and the efficiency of FRET. In order to determine these parameters, three independent signals for the same cell must be measured. The three independent fluorescence signals differ from each other in the wavelength of the excitation or the spectral range of the detection. Because of the different wavelength dependence of the absorption and emission spectra of the donor and acceptor, the corrected transfer signal can be evaluated from the three independently measured parameters, using correction factors determined with the help of single-labeled cells. In this case, biological variations in the level of expression of the investigated protein has no effect on the accuracy of the FRET measurement. The generated distribution histogram of FRET efficiency will provide information about the heterogeneity of the cell population with high statistical accuracy. If there is a change in the FRET efficiency upon stimulus, flow cytometry cannot provide information about the time course of a response in a single cell, but it can easily measure the time course of response in a population of cells. In addition, flow cytometry gives only one value for one cell; the intracellular heterogeneity in FRET efficiency cannot be studied. In many studies, however, the ability of flow cytometry to measure the properties of thousands of cells may be more valuable than detailed information on a smaller number of cells obtained by microscopy. Technical details of how to perform flow cytometric energy transfer measurements can be found in several

recent reviews (Szöllősi and Damjanovich, 1994; Damjanovich et al., 1997; Szöllősi et al., 1998; Szöllősi et al., 2002; Szöllősi and Alexander, 2003; Vereb et al., 2004; Mátýus et al., 2006). Originally, the auto-fluorescence correction for flow cytometric FRET calculations was performed by subtracting a constant value calculated as the average of autofluorescence intensities of the entire cell population from the appropriate fluorescence signals. It should be noted that there is usually a good correlation between the autofluorescence detected in different regions of the spectrum in most cell types, so a more elaborate correction method is also possible. In this method, another independent parameter should be detected, a fourth fluorescence intensity, and this way autofluorescence can be calculated on a cell-by-cell basis (Sebestyén et al., 2002). Naturally, high autofluorescence may decrease the precision of measurements, and therefore it is better to choose fluorophore pairs with long-wavelength emission characteristics, right-shifted from the maximum of the autofluorescence spectrum. Critical parameters influencing the selection of the right FRET donor-acceptor pairs have been discussed recently (Horváth et al., 2005). A versatile computer program for calculating FRET values from flow cytometric data is available (Szentesi et al., 2004). This program is capable of incorporating autofluorescence correction on a cell-by-cell basis.

The obvious advantage of image cytometry is that it yields spatial information at the single-cell level regarding FRET efficiency, a type of information that is not available through other approaches. Resolution of subcellular structures, and analysis of cells *in situ*, can be achieved only by imaging microscopy. Similarly, time-course measurements in single cells can be obtained only by microscopy. Low statistical accuracy is one of the disadvantages of image cytometric FRET measurements, since only a relatively small number of cells can be investigated within a reasonable time frame. The availability of modern digital imaging cameras, as well as associated computer hardware and software, has resulted in rapidly increasing interest in FRET microscopy. These developments have enabled an easy and rapid measurement of fluorescence over  $10^6$  pixels of an image simultaneously. One of the approaches frequently applied in FRET measurements is donor photobleaching. A major advantage of the photobleaching method is that it uses only a single excitation and emission wavelength (Vereb et al., 2004). The

## Flow Cytometry Instrumentation

### 1.12.9

bleaching rate of the donor in the absence of acceptor should be measured under the same experimental conditions as the double-labeled sample, because bleaching rates can vary significantly in different environments. If the efficiency of FRET is relatively low, if the acceptor is nonfluorescent, or if rapid photobleaching prevents measurements of stable fluorescence intensities, the photobleaching method may provide the only practical way to measure FRET efficiency. Because of the destructive nature of the photobleaching method, kinetic measurements of FRET efficiency cannot be performed on the same cell by this method. Intensity-based measurements using the sensitization of acceptor fluorescence can also be used to determine the FRET efficiency on a pixel-by-pixel basis without losing temporal resolution. A thorough comparative analysis of intensity- and donor photobleaching-based FRET microscopic analyses has been carried out (Nagy et al., 1998b). It has been shown that the photobleaching-based method inherently overestimates the FRET efficiency, because this technique weights the FRET efficiency values in single pixels, which is different from the intensity-based energy transfer approach.

Another disadvantage of donor photobleaching FRET is that for calculating FRET efficiency in the double-labeled image on a pixel-by-pixel basis, the photobleaching rate averaged from a donor-only sample must be used. Differences in sample preparation and handling can result in changes in oxygenation and temperature, yielding photobleaching rates that are not comparable across samples. However, combining the method with acceptor photobleaching can improve on this situation in two ways. The procedure to follow is to prepare double-labeled samples, select a region of interest (ROI), and perform the acceptor photobleaching on a part (usually half) of this ROI. This allows calculation of FRET from donor dequenching in this half, which is one advantage of combining the two methods. As an added bonus, in the other half of the ROI, the same calculations should yield a FRET histogram centered at zero, or otherwise enable correction for unwanted donor bleaching during the protocol. The next step is to perform the usual donor photobleaching routine and calculations on the whole ROI. In the acceptor-bleached part, the procedure yields a distribution of the donor photobleaching times without acceptor, which can be used for calculating the FRET image in the double-labeled other half. Although, even in this approach, an average

bleaching time is used for normalization, at least donor bleaching curves in the presence and absence of the acceptor are obtained in the same sample, ROI, and experiment.

It has already been mentioned that the availability of instruments for time-resolved FRET studies is limited because they are sophisticated and expensive. However, significant progress has resulted from the latest developments in this field. Time-resolved fluorescence measurements not only provide an easy way to obtain averaged lifetimes without the exact knowledge of donor concentration, but, more importantly, also give detailed structural information about the donor-acceptor system. The past decade has witnessed tremendous improvements in this area. Picosecond and nanosecond technologies are considered mature now, and commercial instruments are available. Fluorescence decays can be detected by either the single-photon-counting or the phase-modulation method. Both approaches have been successfully applied in spectrofluorimetry; interesting results are summarized in Wu and Brand (1994). Although fluorescence-lifetime measurement based on phase modulation has been available in flow cytometry for years (Steinkamp, 1993), no FRET application has been published so far.

Like spectrofluorimetry, both time-gated and phase-modulated lifetime measurements can be implemented in imaging microscopy. Several nanosecond time-resolved fluorescence images of a sample can be obtained at various delays after pulsed laser excitation of the microscope's entire field of view. Lifetimes are calculated on a pixel-by-pixel basis from these time-resolved images, and the spatial variation of the lifetimes is then displayed. This technique has been used to detect endosome-endosome fusion in single cells (Oida et al., 1993). The other approach, using modulated illumination in microscopy, resulted in successful application of FRET studies for monitoring oligomerization of epidermal growth factor receptors (Gadella and Jovin, 1995). A point calibration procedure to reveal minimum resolved differences (Hanley et al., 2001), as well as a method to avoid photobleaching-related artifacts during phase-modulation lifetime imaging (van Munster and Gadella, 2004), has also been elaborated. Combination of lifetime imaging with programmable array microscopy (PAM) has further improved the quality of lifetime images of samples with multiple fluorophores or spatially varying fluorescence resonance energy transfer efficiency by suppressing

out-of-focus light contributions (Hanley et al., 2005).

One of the latest developments in fluorescence microscopy is spectral imaging, which allows the creation of increasingly complex multicolored samples. Recent improvements in confocal laser scanning microscopy combine sophisticated hardware to obtain fluorescence emission spectra on a single-pixel basis with a mathematical procedure called “linear unmixing” of fluorescence signals. Spectral imaging microscopy has demonstrated substantial superiority over the conventional band-pass filter detection systems with respect to detection accuracy and scale of applicable dye combinations. Spectral imaging has also provided new possibilities for visualizing macromolecular interactions or conformational changes that manifest in altered FRET efficiency (Ecker et al., 2004; Zimmerman, 2005).

## LIMITATIONS OF FRET STUDIES

For proper application of FRET, it is important to understand its limitations as well as its advantages. The most serious drawback of FRET is its modest capacity for determining absolute distances. It is quite good at determining relative distances, namely, whether two points are getting closer or farther apart upon a stimulus. This is caused by the fact that FRET efficiency depends not only on the distance between the donor and acceptor, but also on the relative orientation ( $\kappa^2$ ) of the dyes (see discussion of Theory of FRET). Even when measuring relative distances, care must be taken to ensure that the orientation factor ( $\kappa^2$ ) does not change between the two systems under comparison. In addition, the system can be more complicated when a random conjugation of the fluorescent label is applied. For example, in a substantial fraction of experiments, fluorophore-conjugated monoclonal antibodies are used to label cell-surface antigens. According to common practice, covalent coupling reactions frequently occur between isothiocyanate or succinimidyl ester reactive groups of appropriate derivatives of the fluorophore and the  $\epsilon$ -amino groups of lysine side chains of immunoglobulins. The number of exposed lysine side chains of comparable reactivity found in an antibody molecule usually exceeds one. Each antibody molecule may carry several fluorophores, and the labeled lysine side chains of the individual antibody molecules may be different. Reactive groups are often attached to the fluorophores via an  $n$ -carbon linker, with  $n$  typically ranging

from 2 to 12. The linker often allows relatively free rotation of the dye, which minimizes uncertainty of  $\kappa^2$ . It also minimizes quenching of the dye by the protein, especially if it is due to a hydrophobic environment. The linker, however, has the disadvantage of adding uncertainty to the exact position of the dye. In general, the minimal length that allows free rotation of the dyes and does not cause quenching is around six carbon atoms. More specific labeling of antibodies or antibody fragments can be achieved if SH groups are targeted with maleimide derivatives of fluorophores instead of lysine side chains. In this case, however, the targeted SH group should be introduced into the Fab fragments by genetic modification. Genetically engineered Fab' antibody fragments are designed so that an SH group is introduced on the opposite side of the molecule farthest from the epitope-recognizing portion. Comprehensive FRET studies utilizing combinations of noncompeting Fab' fragments recognizing different epitopes of ErbB2 receptor tyrosine kinase have provided an epitope map of the ErbB2 molecule (Bagossi et al., 2005).

Another problem is that FRET has very sharp distance dependence. For this reason, it is difficult to measure relatively long distances because the signal gets very weak. At the same time, energy transfer tends to be all or none; if the donor and acceptor are within a distance of  $1.63 \times R_0$ , there is energy transfer, but if they are farther apart, energy is transferred with very little efficiency.

When studying cells labeled with donor-and acceptor-conjugated monoclonal antibodies, averaging is performed at different levels. The first averaging follows from the random conjugation of the fluorescent label. An additional averaging is brought about by the eventual distribution of separation distances between the epitopes labeled with monoclonal antibodies. This multiple averaging, an inevitable consequence of the nonuniform stoichiometry, explains why the goal of FRET measurements is different in purified molecular systems and on the surface of the cytoplasmic membrane. In the former case, FRET efficiency values can be converted into absolute distances. Calculation of distance relationships from energy-transfer efficiencies is easy in the case of a single-donor/single-acceptor system if the localization and relative orientation of the fluorophores are known. However, if cell-membrane components are investigated, a two-dimensional restriction applies to the labeled molecules. Analytical solutions for randomly distributed donor and

acceptor molecules and numerical solutions for nonrandom distributions have been elaborated by different groups (Wolber and Hudson, 1979; Dewey and Hammes, 1980; Snyder and Freire, 1982). In order to differentiate between random and nonrandom distributions, energy transfer efficiencies have to be determined at different acceptor concentrations.

## APPLICATIONS

FRET is widely utilized for a variety of applications. In one series of studies, FRET is used to obtain structural information that is otherwise difficult to obtain. The major advantage of FRET for structural studies is that owing to the specificity of labeling the experimental object can be investigated *in situ* and/or *in vivo* with little or no interference from the rest of the system. Even complex and heterogeneous systems can be studied this way. In cytometry, usually cells or cell-like objects, such as ghosts and liposomes, are investigated. FRET applications for liposome fusion or for localization of drugs and membrane proteins in liposomes are reviewed by Szöllősi and Damjanovich (1994). Several reviews are available concerning FRET measurements in biological membranes (Szöllősi and Damjanovich, 1994; Wu and Brand, 1994; Damjanovich et al., 1997; Szöllősi et al., 1998; Szöllősi et al., 2002; Szöllősi and Alexander, 2003; Vereb et al., 2004; Mátyus et al., 2006). These reviews deal with associations of various membrane proteins, structures of receptors, and conformational changes in transmembrane proteins evoked by ligands and membrane potential changes.

In another series of studies, FRET is used as a tool for ensuring high sensitivity of various biological assays. The biotechnological applications of FRET are summarized in reviews that thoroughly discuss working principles of FRET-based enzyme assays and immunoassays, as well as design of tandem dyes and FRET primers for DNA analysis (Clegg, 1995; Szöllősi et al., 1998).

A detailed list of possible FRET applications is beyond the scope of this unit. Readers are referred to the reviews cited above to find useful examples of FRET studies. Here, a few examples are mentioned, demonstrating new and interesting applications of FRET.

Photobleaching FRET measurements have been used to monitor intercellular proximity in order to reveal spatial organization of interacting proteins in the contact region of two cells participating in cytolysis (Bacsó et al., 1996). Interactions between CD8 and major

histocompatibility complex (MHC) class I molecules and between leukocyte function antigen 1 (LFA-1) and intercellular adhesion molecule 1 (ICAM-1) have been investigated using donor (fluorescein)- and acceptor (rhodamine)-labeled monoclonal antibodies. The geometry of the orientation of these proteins based on FRET data was consistent with the observed blocking effects of monoclonal antibodies on the cytolytic activity of killer T lymphocytes (Bacsó et al., 1996).

A steadily expanding new field in FRET studies is based on the application of green fluorescent protein (GFP) as a sensitive reporter. When two differently colored mutants of GFP, such as enhanced green fluorescent protein (EGFP) and enhanced blue fluorescent protein (EBFP), are covalently linked to different intracellular proteins, and these proteins interact with each other, FRET can be detected. Using this approach, spatial and temporal interaction of Bcl-2 and Bax proteins was studied at the single-cell level by monitoring FRET efficiency (Mahajan et al., 1998). Development of different fluorescent protein variants by random mutagenesis has overcome several obstacles such as slow maturation rates, dimerization or oligomerization, sensitivity to environmental ion concentrations, or photobleaching. These improved fluorescent proteins serve as a basis for creating FRET-based intracellular sensors for monitoring cellular concentrations of calcium (Evanko and Haydon, 2005), phosphoinositides (Cicchetti et al., 2004), cGMP (Nikolaev et al., 2006), and membrane potential (Sakai et al., 2001), to mention just a few cellular parameters. Recently, a novel dual FRET fluorescent indicator probe has been developed to monitor the activity of two distinct caspases simultaneously in living cells (Wu et al., 2006). Quantitation of FRET efficiency calculated between GFP variants often poses a problem in flow cytometric measurements. Therefore, chimeras in which the cyan fluorescent protein was separated by amino acid linkers of different lengths from the yellow fluorescent protein were generated and used to calibrate flow cytometric FRET measurements. Calibration was achieved by calculating the FRET efficiency in two different ways and minimizing the squared differences between the two results by changing the appropriate spectral parameter (Nagy et al., 2005).

A new extension of the application of GFP proteins in FRET studies has been achieved by combining GFP with luciferase. Bioluminescent resonance energy transfer (BRET) uses bioluminescent luciferase that is genetically

fused to one candidate protein and a GFP mutant, enhanced yellow fluorescent protein (EYFP), fused to another protein of interest. If the two fusion proteins come close enough, resonance energy transfer can occur, resulting in changes in the spectrum of the bioluminescent emission. The BRET method was used to assay interactions between proteins encoded by the circadian clock genes *kaiA* and *kaiB* in cyanobacterium (Xu et al., 1999). The BRET technique has been applied to detect the association state of the melanocortin receptor. Toward this end, melanocortin receptors were fused with either modified GFP or *Renilla* luciferase at their C terminus. BRET assays revealed that the melanocortin 4 receptor exists as a constitutive homodimer, which is not regulated by peptide interaction (Nickolls and Maki, 2006).

A single-molecule fluorescence resonance energy transfer (FRET) method has been developed to observe the activation of the small G protein Ras at the level of individual molecules. Human epidermoid mouth carcinoma (KB) cells expressing H- or K-Ras fused with YFP (donor) were microinjected with the fluorescent GTP analog Bodipy TR-GTP (acceptor), and the epidermal growth factor-induced binding of Bodipy TR-GTP to YFP-(H or K)-Ras was monitored by single-molecule FRET using total internal reflection microscopy. On activation, Ras diffusion was greatly suppressed/immobilized, suggesting the formation of large, activated Ras-signaling complexes. These complexes may work as platforms for transducing the Ras signal to effector molecules, further suggesting that Ras signal transduction requires more than simple collisions with effector molecules (Murakoshi et al., 2004).

FRET data and molecular modeling can be combined to provide hints about possible orientation and arrangements of membrane proteins. Recently a model has been proposed for the nearly full-length ErbB2 using FRET measurements, crystal structures of the ErbB2 ectodomain, and molecular modeling methods. Using fluorescently labeled Fab' antibody fragments recognizing different epitopes of the ErbB2 receptor tyrosine kinase, the proximity of the ErbB2 ectodomain to the cell membrane has been determined by FRET measurements. Interestingly, in this case the rate of FRET efficiency depends upon the fourth power of the distance between the epitope and the plane of the membrane, because of the two-dimensional restriction of the acceptor molecule incorporated into the cell membrane.

It has been concluded that ErbB2 molecules form homodimers, and the modeling has revealed a structure possessing three potential interacting regions (Bagossi et al., 2005).

Since Förster first established the analysis of FRET phenomena in 1946, the number of applications of FRET has increased enormously in various fields of research and biotechnology. Technical improvements in spectrofluorimeters, flow cytometers, and microscopes, as well as introduction of new fluorescent probes with better photophysical properties, open up new areas for employing the FRET method innovatively and successfully.

## LITERATURE CITED

- Bacsó, Z., Bene, L., Bodnár, A., Matkó, J., and Damjanovich, S. 1996. A photobleaching energy transfer analysis of CD8/MHC-I and LFA-1/ICAM-1 interactions in CTL-target cell conjugates. *Immunol. Lett.* 54:151-156.
- Bagossi, P., Horváth, G., Vereb, G., Szöllősi, J., and Tózsér, J. 2005. Molecular modeling of nearly full-length ErbB2 receptor. *Biophys. J.* 88:1354-1363.
- Bastiaens, P.I.H. and Jovin, T.M. 1996. Microspectroscopic imaging tracks the intracellular processing of a signal transduction protein: Fluorescent-labeled protein kinase C $\beta$ I. *Proc. Natl. Acad. Sci. U.S.A.* 93:8407-8412.
- Bastiaens, P.I.H., Majoul, I.V., Verveer, P.J., Söling, H.-D., and Jovin, T.M. 1996. Imaging the intracellular trafficking and state of the AB<sub>5</sub> quaternary structure of cholera toxin. *EMBO J.* 15:4246-4253.
- Bene, L., Szöllősi, J., Szentesi, G., Damjanovich, L., Gáspár, R. Jr., Waldmann, T.A., and Damjanovich, S. 2005. Detection of receptor trimers on the cell surface by flow cytometric fluorescence energy homotransfer measurements. *Biochim. Biophys. Acta.* 1744:176-198.
- Bhatia, S., Edidin, M., Almo, S.C., and Nathenson, S.G. 2005. Different cell surface oligomeric states of B7-1 and B7-2: Implications for signaling. *Proc. Natl. Acad. Sci. U.S.A.* 102:15569-15574.
- Carraway, K.L. III., Koland, J.G., and Cerione, R.A. 1989. Visualization of epidermal growth factor (EGF) receptor aggregation in plasma membranes by fluorescence resonance energy transfer. *J. Biol. Chem.* 264:8699-8707.
- Cemerski, S. and Shaw, A. 2006. Immune synapses in T-cell activation. *Curr. Opin. Immunol.* 18:298-304.
- Chen, R.F. and Knutson, J.R. 1988. Mechanism of fluorescence concentration quenching of carboxyfluorescein in liposomes: Energy transfer to nonfluorescent dimers. *Anal. Biochem.* 172:61-77.
- Cicchetti, G., Biernacki, M., Farquharson, J., and Allen, P.G. 2004. A ratiometric expressible FRET sensor for phosphoinositides displays a signal change in highly dynamic membrane

- structures in fibroblasts. *Biochemistry* 43:1939-1949.
- Clegg, R.M. 1995. Fluorescence resonance energy transfer. *Curr. Opin. Biotechnol.* 6:103-110.
- Crissman, H.A. and Steinkamp, J.A. 2001. Flow cytometric fluorescence lifetime measurements. *Methods Cell Biol.* 63:131-148.
- Dale, R.E., Eisinger, J., and Blumberg, W.E. 1979. The orientational freedom of molecular probes: The orientation factor in intramolecular energy transfer. *Biophys. J.* 26:161-194.
- Damjanovich, S., Gáspár, R., and Pieri, C. 1997. Dynamic receptor superstructure at plasma membrane. *Q. Rev. Biophys.* 30:67-106.
- Dewey, T.G. and Hammes, G.G. 1980. Calculation of fluorescence resonance energy transfer on surfaces. *Biophys. J.* 32:1023-1035.
- Ecker, R.C., de Martin, R., Steiner, G.E., and Schmid, J.A. 2004. Application of spectral imaging microscopy in cyomics and fluorescence resonance energy transfer (FRET) analysis. *Cytometry A* 59:172-181.
- Evanko, D.S. and Haydon, P.G. 2005. Elimination of environmental sensitivity in a cameleon FRET-based calcium sensor via replacement of the acceptor with Venus. *Cell Calcium* 37:341-348.
- Förster, T. 1946. Energiewanderung und Fluoreszenz. *Naturwissenschaften* 6:166-175.
- Förster, T. 1948. Zwischenmolekulare Energiewanderung und Fluoreszenz. *Ann. Phys. (Leipzig)* 2:55-75.
- Gadella, T.W.J. and Jovin, T.M. 1995. Oligomerization of epidermal growth factor receptors on A431 cells studied by time-resolved fluorescence imaging microscopy: A stereochemical model for tyrosine kinase receptor activation. *J. Cell Biol.* 129:1543-1558.
- Gettins, P., Beechem, J.M., Crews, B.C., and Cunningham, L.W. 1990. Separation and localization of the four cysteine-949 residues in human  $\beta$ 2-macroglobulin using fluorescence energy transfer. *Biochemistry* 29:7747-7753.
- Ha, T., Enderle, Th., Odletree, D.F., Chemla, D.S., Selvin, P.R., and Weiss, S. 1996. Probing the interaction between two single molecules: Fluorescence resonance energy transfer between a single donor and a single acceptor. *Proc. Natl. Acad. Sci. U.S.A.* 93:6264-6268.
- Hanley, Q.S., Subramaniam, V., Arndt-Jovin, D.J., and Jovin, T.M. 2001. Fluorescence lifetime imaging: Multi-point calibration, minimum resolvable differences, and artifact suppression. *Cytometry* 43:248-260.
- Hanley, Q.S., Lidke, K.A., Heintzmann, R., Arndt-Jovin, D.J., and Jovin, T.M. 2005. Fluorescence lifetime imaging in an optically sectioning programmable array microscope (PAM). *Cytometry A* 67:112-118.
- Horváth, G., Petrás, M., Szentesi, G., Fábián, A., Park, J.W., Vereb, G., and Szöllősi, J. 2005. Selecting the right fluorophores and flow cytometer for fluorescence resonance energy transfer measurements. *Cytometry A* 65:148-157.
- Jares-Erijman, E.A. and Jovin, T.M. 2003. FRET imaging. *Nat. Biotechnol.* 21:1387-1395.
- Johnson, D.A., Leathers, V.L., Martinez, A.M., Walsh, D.A., and Fletcher, W.H. 1993. Fluorescence resonance energy transfer within a heterochromatic cAMP-dependent protein kinase holoenzyme under equilibrium conditions: New insights into the conformational changes that result in cAMP-dependent activation. *Biochemistry* 32:6402-6410.
- Jovin, T.M. and Arndt-Jovin, D.J. 1989a. Luminescence digital imaging microscopy. *Ann. Rev. Biophys. Biophys. Chem.* 18:271-308.
- Jovin, T.M. and Arndt-Jovin, D.J. 1989b. FRET microscopy: Digital imaging of fluorescence resonance energy transfer: Application in cell biology. In *Microspectrofluorometry of Single Living Cells* (E. Kohen, J.S. Ploem, and J.G. Hirschberg, eds.) pp. 99-117. Academic Press, Orlando.
- Kosk-Kosicka, D., Bzdega, T., and Wawrynow, A. 1989. Fluorescence energy transfer studies of purified erythrocyte  $\text{Ca}^{2+}$ -ATPase  $\text{Ca}^{2+}$ -regulated activation by oligomerization. *J. Biol. Chem.* 264:19495-19499.
- Lidke, D.S., Nagy, P., Barisas, B.G., Heintzmann, R., Post, J.N., Lidke, K.A., Clayton, A.H., Arndt-Jovin, D.J., and Jovin, T.M. 2003. Imaging molecular interactions in cells by dynamic and static fluorescence anisotropy (rFLIM and emFRET). *Biochem. Soc. Trans.* 31:1020-1027.
- MacDonald, R.I. 1990. Characteristics of self-quenching of the fluorescence of lipid-conjugated rhodamine in membranes. *J. Biol. Chem.* 265:13533-13539.
- Mahajan, N.P., Linder, K., Berry, G., Gordon, G.W., Heim, R., and Herman, B. 1998. Bcl-2 and Bax interactions in mitochondria probed with green fluorescent protein and fluorescence resonance energy transfer. *Nature Biotechnol.* 6:547-552.
- Maliwal, B.P., Kusba, J., and Lakowicz, J.R. 1995. Fluorescence energy transfer in one dimension: Frequency-domain fluorescence study of DNA-fluorophore complexes. *Biopolymers* 35:245-255.
- Mathis, G. 1993. Rare earth cryptates and homogeneous fluoroimmunoassays with human sera. *Clin. Chem.* 39:1953-1959.
- Matkó, J., Jenei, A., Mátyus, L., Ameloot, M., and Damjanovich, S. 1993. Mapping of cell surface protein-patterns by combined fluorescence anisotropy and energy transfer measurements. *J. Photochem. Photobiol. B Biol.* 19:69-73.
- Mátyus, L. 1992. Fluorescence resonance energy transfer measurements on cell surfaces: A spectroscopic tool for determining protein interactions. *J. Photochem. Photobiol. B Biol.* 12:323-337.
- Mátyus, L., Szöllősi, J., and Jenei, A. 2006. Steady-state fluorescence quenching applications for studying protein structure and dynamics. *J. Photochem. Photobiol. B* 83:223-236.

- Mekler, V.M. 1997. A photochemical technique to enhance sensitivity of detection of fluorescence resonance energy transfer. *Photochem. Photobiol.* 59:615-620.
- Murakoshi, H., Iino, R., Kobayashi, T., Fujiwara, T., Ohshima, C., Yoshimura, A., and Kusumi, A. 2004. Single-molecule imaging analysis of Ras activation in living cells. *Proc. Natl. Acad. Sci. U.S.A.* 101:7317-7322.
- Nagy, P., Bene, L., Balázs, M., Hyun, W.C., Lockett, S.J., Chiang, N.Y., Waldman, F., Feuerstein, B.G., Damjanovich, S., and Szöllősi, J. 1998a. EGF-induced redistribution of erbB2 on breast tumor cells: Flow and image cytometric energy transfer measurements. *Cytometry* 32:120-131.
- Nagy, P., Vámosi, G., Bodnár, A., Lockett, S.J., and Szöllősi, J. 1998b. Intensity-based energy transfer measurements in digital imaging microscopy. *Eur. Biophys. J.* 27:377-389.
- Nagy, P., Bene, L., Hyun, W.C., Vereb, G., Braun, M., Antz, C., Paysan, J., Damjanovich, S., Park, J.W., and Szöllősi, J. 2005. Novel calibration method for flow cytometric fluorescence resonance energy transfer measurements between visible fluorescent proteins. *Cytometry A* 67:86-96.
- Nickolls, S.A. and Maki, R.A. 2006. Dimerization of the melanocortin 4 receptor: A study using bioluminescence resonance energy transfer. *Peptides* 27:380-387.
- Nikolaev, V.O., Gambaryan, S., and Lohse, M.J. 2006. Fluorescent sensors for rapid monitoring of intracellular cGMP. *Nat. Methods* 3:23-25.
- Oida, T., Sako, Y., and Kusumi, A. 1993. Fluorescence lifetime imaging microscopy (flimscopy): Methodology development and application to studies of endosome fusion in single cells. *Biophys. J.* 64:676-685.
- Ozinskas, A.J., Malak, H., Joshi, J., Szmacinski, H., Britz, J., Thompson, R.B., Koen, P.A., and Lakowicz, J.R. 1993. Homogeneous model immunoassay of thyroxin by phase modulation fluorescence spectroscopy. *Anal. Biochem.* 213:264-270.
- Patterson, G.H., Piston, D.W., and Barisas, B.G. 2000. Förster distances between green fluorescent protein pairs. *Anal. Biochem.* 284:438-440.
- Sakai, R., Repunte-Canonigo, V., Raj, C.D., and Knopfel, T. 2001. Design and characterization of a DNA-encoded, voltage-sensitive fluorescent protein. *Eur. J. Neurosci.* 13:2314-2318.
- Sebestyén, Z., Nagy, P., Horváth, G., Vámosi, G., Debets, R., Gratama, J.W., Alexander, D.R., and Szöllősi, J. 2002. Long wavelength fluorophores and cell-by-cell correction for autofluorescence significantly improves the accuracy of flow cytometric energy transfer measurements on a dual-laser benchtop flow cytometer. *Cytometry* 48:124-135.
- Shahrokh, Z., Verkman, A.S., and Shohet, S.B. 1991. Distance between skeletal protein 4.1 and the erythrocyte membrane bilayer measured by resonance energy transfer. *J. Biol. Chem.* 266:12082-12089.
- Snyder, B. and Freire, E. 1982. Fluorescence energy transfer in two dimensions: A numeric solution for random and nonrandom distributions. *Bioophys. J.* 40:137-148.
- Steinkamp, J.A. and Crissman, H.A. 1993. Resolution of fluorescence signals from cells labeled with fluorochromes having different lifetimes by phase-sensitive flow cytometry. *Cytometry* 14:210-216.
- Stryer, L. 1978. Fluorescence energy transfer as a spectroscopic ruler. *Annu. Rev. Biochem.* 47:819-846.
- Szentesi, G., Horváth, G., Bori, I., Vámosi, G., Szöllősi, J., Gáspár, R., Damjanovich, S., Jenei, A., and Mátyus, L. 2004. Computer program for determining fluorescence resonance energy transfer efficiency from flow cytometric data on a cell-by-cell basis. *Comput. Methods Programs Biomed.* 75:201-211.
- Szentesi, G., Vereb, G., Horváth, G., Bodnár, A., Fábián, Á., Matkó, J., Gáspár, R., Damjanovich, S., Mátyus, L., and Jenei, A. 2005. Computer program for analyzing donor photobleaching FRET image series. *Cytometry* 67A:119-128.
- Szöllősi, J. and Alexander, D.R. 2003. The application of fluorescence resonance energy transfer to the investigation of phosphatases. *Methods Enzymol.* 366:203-224.
- Szöllősi, J. and Damjanovich, S. 1994. Mapping of membrane structures by energy transfer measurements. In *Mobility and Proximity in Biological Membranes*. (S. Damjanovich, J. Szöllősi, L. Trón, and M. Edidin, eds.) pp. 49-108. CRC Press, Boca Raton, Fla.
- Szöllősi, J., Nagy, P., Sebestyén, Z., Damjanovich, S., Park, J.W., and Mátyus, L. 2002. Applications of fluorescence resonance energy transfer for mapping biological membranes. *J. Biotechnol.* 82:251-266.
- Szöllősi, J., Szabó, G., Somogyi, B., and Damjanovich, S. 1978. Simultaneous fluorescence labeling of human fibroblast cells with fluorescamine and propidium iodide. *Acta Biochem. Biophys. Acad. Sci. Hung.* 13:63-66.
- Szöllősi, J., Trón, L., Damjanovich, S., Helliwell, S.H., Arndt-Jovin, D.J., and Jovin, T.M. 1984. Fluorescence energy transfer measurements on cell surfaces: A critical comparison of steady-state and flow cytometric methods. *Cytometry* 5:210-216.
- Szöllősi, J., Damjanovich, S., and Mátyus, L. 1998. Application of fluorescence resonance energy transfer in the clinical laboratory: Routine and research. *Cytometry* 34:159-179.
- Taylor, D.L., Reidler, J., Spudich, J.A., and Stryer, L. 1981. Detection of actin assembly by fluorescence energy transfer. *J. Cell. Biol.* 89:362-367.
- Trón, L. 1994. Experimental methods to measure fluorescence resonance energy transfer. In *Mobility and Proximity in Biological Membranes*. (S. Damjanovich, J. Szöllősi, L. Trón, and M. Edidin, eds.) pp. 1-47. CRC Press, Boca Raton, Fla.

- van Munster, E.B. and Gadella, T.W. Jr. 2004. Suppression of photobleaching-induced artifacts in frequency-domain FLIM by permutation of the recording order. *Cytometry A* 58:185-194.
- Vereb, G., Meyer, C.K., and Jovin, T.M. 1997. Novel microscope-based approaches for the investigation of protein-protein interactions in signal transduction. In *Interacting Protein Domains: Their Role in Signal and Energy Transduction*. Volume 102, NATO ASI Series, H:Cell Biology. (L.M.G. Heilmeyer, ed.) pp. 49-52. Springer Verlag, Berlin.
- Vereb, G., Matkó, J., and Szöllősi, J. 2004. Cytometry of fluorescence resonance energy transfer. *Methods Cell Biol.* 75:105-152.
- Waharte, F., Spriet, C., and Heliot, L. 2006. Setup and characterization of a multiphoton FLIM instrument for protein-protein interaction measurements in living cells. *Cytometry A*. 69:299-306.
- Wallrabe, H. and Periasamy, A. 2005. Imaging protein molecules using FRET and FLIM microscopy. *Curr. Opin. Biotechnol.* 16:19-27.
- Wolber, P.K. and Hudson, B.S. 1979. An analytic solution to the Förster energy transfer problem in two dimensions. *Biophys. J.* 28:197-210.
- Wolf, D.E., Winiski, A.P., Ting, A.E., Bocian, K.M., and Pagano, R.E. 1992. Determination of the transbilayer distribution of fluorescent lipid ana-
- logues by nonradiative fluorescence resonance energy transfer. *Biochemistry* 31:2865-2873.
- Wu, P. and Brand, L. 1994. Resonance energy transfer: Methods and applications. *Anal. Biochem.* 218:1-13.
- Wu, X., Simone, J., Hewgill, D., Siegel, R., Lipsky, P.E., and He, L. 2006. Measurement of two caspase activities simultaneously in living cells by a novel dual FRET fluorescent indicator probe. *Cytometry A* 69:477-486.
- Xu, Y., Piston, D.W., and Johnson, C.H. 1999. A bioluminescence resonance energy transfer (BRET) system: Application to interacting circadian clock proteins. *Proc. Natl. Acad. Sci. U.S.A.* 96:151-156.
- Yamazaki, I., Tamai, N., and Yamazaki, T. 1990. Electronic excitation transfer in organized molecular assemblies. *J. Phys. Chem.* 94:516-525.
- Zimmermann, T. 2005. Spectral imaging and linear unmixing in light microscopy. *Adv. Biochem. Eng. Biotechnol.* 95:245-265.

---

Contributed by János Szöllősi, Sándor Damjanovich, Péter Nagy, György Vereb, and László Mátyus  
University Medical School of Debrecen  
Debrecen, Hungary

*The authors wish to acknowledge support by the Hungarian Academy of Sciences (grant numbers: OTKA F049025, T043509, T043061, K626h8), the Péter Pázmány Program for Regional Knowledge Centers (contract number: 06/2004), and the European Commission (contract numbers: LSHC-CT-2005-018914, LSHB-CT-2004-503467, MRTN-CT-2005-019h81, MRTN-CT-2006-035946-2).*